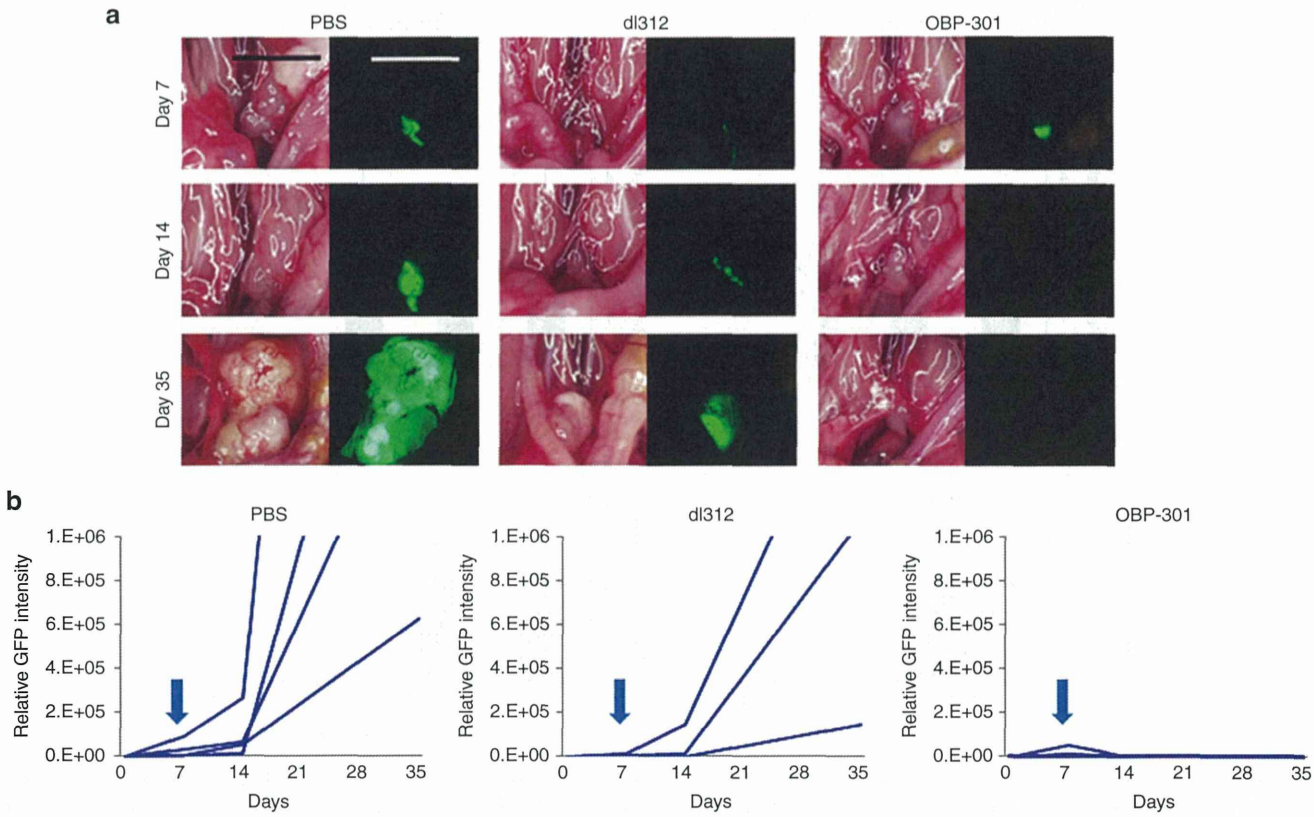

Figure 6 Virus-mediated biological elimination of established lymph node metastasis prevented relapse. (**a**) Gross and fluorescence images of the abdominal cavity were serially obtained at laparotomy on days 7, 14, and 35 after tumor inoculation in orthotopic HCT-116-GFP tumor xenografts treated with PBS, dl312, or OBP-301. Representative images of each group are shown. Scale bar, 5 mm. (**b**) The GFP intensity of metastatic lymph nodes in each mouse was serially measured on days 7, 14, and 35. Data from each mouse are plotted individually. Arrows indicate the time of virus injection and primary tumor removal.

Overexpression of telomerase, which is a ribonucleoprotein enzyme complex that is responsible for the complete replication of chromosomal ends, is thought to play a key role in the infinite reproduction of cancer cells.[27,28] We constructed a telomerase-specific replicating adenovirus, OBP-301, in which the hTERT promoter element drives expression of the *E1* genes that are essential for adenoviral replication.[19] As hTERT is the catalytic subunit of telomerase, OBP-301 shows tumor-specific intracellular viral replication that is regulated by hTERT transcriptional activity in human tumors.[19–21] Viral yields correlated well with *hTERT* mRNA expression in human cancer cell lines,[13,22] although there was no significant correlation between *hTERT* mRNA expression and the cytopathic activity of OBP-301.[21] It has been reported that the hTERT promoter could be applied to induction of transgene expression in syngeneic tumors in mice.[29] We also previously confirmed that a hTERT promoter-driven tumor-killing adenovirus could replicate in murine colorectal cancer cells such as Colon-26 *in vitro* and *in vivo*.[13] These findings suggest that OBP-301 can replicate in murine as well as in human tissues, when telomerase is activated. Thus, the submucosally invaded orthotopic early rectal cancer mouse model, which develops spontaneous lymph node metastasis, is a suitable translational animal model for simulation of the *in vivo* behavior patterns of this virus.

The lymphatic system plays a crucial role in initial lymphatic dissemination of human cancer cells and subsequent development of lymph node metastases. In addition to the pre-existing lymphatic network, it is well known that new lymphatic vessels can be generated from pre-existing ones by tumor-secreting mediators such as vascular endothelial growth factors (VEGF) and angiopoietins.[30] This tumor-induced lymphangiogenesis is often associated with structural and functional abnormalities of the lymphatic vasculature, which are analogous to the aberrations of tumor blood vessels.[31] Although lymphatic vessels began to show abnormalities even in the early stages of carcinogenesis, advanced tumors have more compressed and nonfunctional lymphatics presumably due to tumor infiltration.[32] The lymphatic system also provides a route for the delivery of therapeutic molecules including biological agents. We have shown that OBP-301 virus injected into the space under the orthotopically implanted early rectal cancer could easily reach regional lymph nodes with normal lymphatic flow. However, a complex and impaired lymphatic network in more advanced tumors might disturb an optimal distribution of therapeutics into the regional lymphatic area. Therefore, early-stage cancer patients who potentially have microlymph node metastasis might be an appropriate target for locoregional therapy through the lymphatic system.

The standard procedures for ESD, which include marking outside the lesion, injection of various submucosal solutions, circumferential incision into the mucosa and direct dissection of the submucosal layer, have been established.[33] As submucosal

dissection with simultaneous hemostasis causes destruction of the normal lymphatic network, administration of therapeutic molecules prior to complete removal of neoplastic lesions is the ideal time to deliver these molecules over the locoregional lymphatic area including the sentinel lymph nodes. The use of submucosal injection to isolate the target lesion is considered to be essential for a successful ESD. In addition to normal saline, many types of solutions such as glycerol, dextrose water, and hyaluronic acid have been applied clinically.[34] The key aspect of our study is that a solution containing tumor-killing virus was used as a submucosal cushion and, therefore, the virus delivery could be easily adapted to the standard ESD procedures. Moreover, we found that submucosally injected dye could rapidly enter the lymphatic flow and spread to the draining lymph nodes, indicating a potential for extension of the purging effects of the viruses beyond the sentinel lymph nodes.

Submucosal injection of OBP-301 prior to ESD-mimicking resection of submucosally invaded primary tumors resulted in complete inhibition of metastatic outgrowth on the draining lymph nodes in a dose-dependent manner. Replicating viruses in metastatic foci of the sentinel lymph nodes could be visualized using dual-color *in vivo* imaging. Preclinical studies have demonstrated that the antitumor efficiency of OBP-301 strongly depends on its infectivity towards tumor cells, which varies among tumor types.[21,35] However, a dose-titration study indicated that OBP-301 at 10^7 PFU, which is 2 logs lower than the optimal concentration for mice (1×10^9 PFU/mouse), could still effectively suppress lymph node metastasis, suggesting that the use of higher doses of OBP-301 could potentially overcome the varied sensitivity of tumor cells to OBP-301. The safety profile of OBP-301 itself after intratumoral delivery has already been confirmed up to 1×10^{12} virus particles (vp) (1×10^{11} PFU) in a phase 1 clinical trial for various types of solid tumors.[36] Furthermore, an investigator-driven clinical study of OBP-301 in combination with radiotherapy for esophageal cancer is currently ongoing in our hospital without any severe dose-limiting toxicity. Therefore, a 2-log-higher dose of OBP-301 could be available in humans for monotherapy as well as for combination therapy. In addition, analysis of autopsied patients in our previous trial showed that a replication-defective adenoviral vector can persist in proximal lymph nodes for ~5 months after intratumoral injection.[37] Indeed, although metastatic lymph nodes grew in mice that received cisplatin, which is a broadly used anticancer drug, no recurrence was observed in OBP-301–treated mice in which lymph node metastasis had been eradicated, suggesting a long-term surveillance activity of OBP-301.

In conclusion, we have demonstrated that the telomerase-specific replication-selective adenovirus OBP-301 can be delivered into neoplastic foci in regional lymph nodes after submucosal injection at the time of primary tumor dissection and effectively ablate lymph node metastasis in an early gastrointestinal cancer model. We previously reported that metastatic tumor cells in the lymph nodes unexpectedly increased after surgical removal of invasive rectal tumors, presumably due to excessive damage to the host[38]; however, less-invasive submucosal dissection of tumors did not affect the incidence of lymph node metastasis. The administration of OBP-301 by inclusion in the standard ESD procedures is a revolutionary treatment option for early gastrointestinal cancer patients, which avoids impairing the quality of life that occurs due to surgery for prophylactic lymphadenectomy. Moreover, clinical morbidity of lymphedema particularly in breast cancer axillary node dissection is of significant consequence. Our strategy may have a potential for clinical advantages in other oncologic fields.

MATERIALS AND METHODS

Cell lines and recombinant adenoviruses. The human colorectal cancer cell lines HCT-116-GFP and Colo 205-GFP, which express the *GFP* gene, and HCT-116-red fluorescent protein (RFP) cells, which express the *RFP* gene, were established previously,[39–42] and were routinely cultured in RPMI 1640 medium supplemented with 10% FBS. The recombinant replication-selective, tumor-specific adenovirus vector OBP-301 (Telomelysin), in which the hTERT promoter element drives the expression of *E1A* and *E1B* genes linked with an internal ribosome entry site, was previously constructed and characterized[19–21] (**Supplementary Figure S1a**). OBP-401 (TelomeScan) is a telomerase-specific, replication-competent adenovirus variant in which the replication cassette and *GFP* gene under the control of the cytomegalovirus promoter were inserted into the E3 region for monitoring of viral replication[13,22] (**Supplementary Figure S1b**). The E1A-deleted adenovirus vector lacking a cDNA insert (dl312) was also used as a control vector. Viruses were purified by ultracentrifugation using CsCl step gradients. Viral titers were determined by a plaque-forming assay using 293 cells. The virus was stored at −80 °C.

Cell viability assay. HCT-116-GFP and Colo 205-GFP cells were seeded on 96-well plates at a density of 1×10^3 cells/well 18–20 hours before viral infection. The cells were then infected with OBP-301 or control dl312 at an MOI of 0, 1, 5, 10, 50, or 100 PFU/cell. Cell viability was determined on days 1, 2, 3, and 5 after virus infection using the Cell Proliferation Kit II (Roche Molecular Biochemicals, Indianapolis, IN), which is based on a sodium 3′-[1-(phenylaminocarbonyl)-3,4-tetrazolium]-bis(4-methoxy-6-nitro)benzene sulfonic acid hydrate (XTT) assay, according to the manufacturer's protocol.

Animal experiments. The experimental protocol was approved by the Ethics Review Committee for Animal Experimentation of our institution. Six- to 8-week-old, female BALB/c nude mice (Clea Japan, Tokyo, Japan) were used in this study. All animal procedures were performed under anesthesia using s.c. administration of a ketamine mixture (100 mg/kg ketamine HCL, 7 mg/kg xylazine HCL).

Mice were anesthetized and placed in a supine position. Both the dorsal vaginal wall and the ventral ano-rectal wall were cut at a length of 7 mm to expose the rectal mucosa for an easy operation. To develop a submucosally invaded orthotopic rectal cancer model, HCT-116-GFP, Colo205-GFP, or HCT-116-RFP human colon cancer cells (1.5×10^6 cells/mouse), suspended in a mixture of 15 μl of PBS and 15 μl of Matrigel (BD Biosciences, San Jose, CA), were slowly injected into the submucosal layer of the rectum using a 30-gauge needle (**Supplementary Figure S3**). Seven days later, after fluorescent signals were confirmed in the sentinel lymph nodes at laparotomy, a 30 μl-solution containing OBP-301, OBP-401, or dl312 at the indicated doses was peritumorally injected into the submucosal space as a fluid cushion. The minute GFP- or FRP-positive rectal tumors were then surgically removed.

For pathological evaluation of lymph node metastasis, mice were sacrificed and all para-aortic or iliac lymph nodes were isolated and were stained with hematoxylin and eosin or were immunohistochemically analyzed.

In vivo *fluorescence imaging.* To monitor the outgrowth of the primary tumors and the metastatic lymph nodes, *in vivo* fluorescence images were obtained at laparotomy using an Olympus SZX16 microscope and a DP71

camera (Olympus, Tokyo, Japan). Images were processed for contrast and brightness with the use of Adobe Photoshop software (Adobe). Green fluorescence intensity was analyzed using Image J software for the quantification of lymph node metastasis. For long-term evaluation, abdominal images were serially obtained and quantified.

Quantitative real-time PCR analysis. We previously established a highly sensitive quantitative assay that targets a human-specific *Alu* sequence in order to quantify lymph node metastasis in mice. We used this previously described assay in this study to measure the number of metastatic human tumor cells in mouse lymph nodes[38]. Briefly, genomic DNA was extracted from harvested lymph node tissues and analyzed by the quantitative real-time PCR assay using a set of human *Alu* primers (sense: 5′-CTG AGG TCA GGA GTT CGA G-3′; and antisense: 5′-TCA AGC GAT TCT CCT GCC-3′). We also amplified the mouse *GAPDH* genomic DNA sequence using mouse *GAPDH* primers (sense: 5′-CCA CTC TTC CAC CTT CGA T-3′; and antisense: 5′-CAC CAC CCT GTT GCT GTA-3′). The number of metastatic tumor cells in mouse lymph nodes is defined as the *Alu*/*GAPDH* ratio relative to that of the PBS-treated sample (PBS = 1).

Immunohistochemistry. For histological studies, rectal tumors and lymph nodes were removed and placed into buffered formalin for 24 hours at room temperature. All of the tissues were subsequently processed through alcohol dehydration and paraffinization. Tissues were embedded in paraffin and sectioned for hematoxylin-eosin staining and also for immunohistochemical examination. After deparaffinization and rehydration, antigen retrieval was performed by microwave irradiation in 10 mmol/l citrate buffer (pH 6.0). Following quenching of endogenous tissue peroxidase, tissue sections were incubated with mouse anti-adenovirus type 5 E1AmAb (BD Biosciences). The sections were then incubated using the Histofine Mouse Stain Kit (Nichirei Biosciences, Tokyo, Japan) for 10 minutes at 25 °C to block nonspecific reactivity with mouse serum. Immunoreactive signals were visualized by using a 3,39-diaminobenzidine tetrahydrochloride solution, and the nuclei were counterstained with hematoxylin. Signals were viewed under a microscope (BX50; Olympus).

Statistical analysis. We used Student's *t*-test to identify statistically significant differences between groups. All data are expressed as means ± SD. *P* values less than 0.05 were considered statistically significant.

SUPPLEMENTARY MATERIAL

Figure S1. Schematic DNA structures of the telomerase-specific viruses.

Figure S2. *In vitro* cytopathic effect of OBP-301 on Colo205-GFP human colorectal cancer cells..

Figure S3. Procedure for inoculation of human colorectal cancer cells for establishment of a submucosally invaded orthotopic xenograft model.

Figure S4. *In vivo* lymphatic spread of a blue dye in the regional lymph nodes.

Figure S5. Removal of the primary rectal tumor mimicking endoscopic submucosal dissection (ESD).

Figure S6. Comparative study of OBP-301 and cisplatin effects in an orthotopic colorectal cancer xenograft model.

ACKNOWLEDGMENTS

We thank Tomoko Sueishi and Tae Yamanishi for their excellent technical support. We also thank Yoshiko Mori and Ryo Inada for helpful discussions. This work was supported in part by grants from The Mochida Memorial Foundation for Medical and Pharmaceutical Research (H.K.); The Kanae Foundation for the Promotion of Medical Science (H.K.); The 106th Annual Congress of the JSS Memorial Surgical Research Fund, Tokyo, Japan (H.K.) Young Scientists (B), The Ministry of Education, Culture, Sports, Science and Technology, Japan (H.K.), the Ministry of Education, Culture, Sports, Science, and Technology of Japan (T.F.) and the Ministry of Health, Labour and Welfare of Japan (T.F.). Y.U. is the president and CEO of Oncolys BioPharma, Inc., the manufacturer of viruses. H.T. and T.F. are consultants for Oncolys BioPharma, Inc. The other authors declare no conflict of interest.

REFERENCES

1. Yamamoto, H, Koiwai, H, Yube, T, Isoda, N, Sato, Y, Sekine, Y *et al.* (1999). A successful single-step endoscopic resection of a 40 millimeter flat-elevated tumor in the rectum: endoscopic mucosal resection using sodium hyaluronate. *Gastrointest Endosc* **50**: 701–704.
2. Repici, A, Hassan, C, De Paula Pessoa, D, Pagano, N, Arezzo, A, Zullo, A *et al.* (2012). Efficacy and safety of endoscopic submucosal dissection for colorectal neoplasia: a systematic review. *Endoscopy* **44**: 137–150.
3. Montgomery, M, Fukuhara, S, Karpeh, M and Brower, S (2013). Evidence-based review of the management of early gastric cancer. *Gastroenterol Rep (Oxf)* **1**: 105–112.
4. Volk, EE, Goldblum, JR, Petras, RE, Carey, WD and Fazio, VW (1995). Management and outcome of patients with invasive carcinoma arising in colorectal polyps. *Gastroenterology* **109**: 1801–1807.
5. Kudo, S, Kashida, H, Nakajima, T, Tamura, S and Nakajo, K (1997). Endoscopic diagnosis and treatment of early colorectal cancer. *World J Surg* **21**: 694–701.
6. Mainprize, KS, Mortensen, NJ and Warren, BF (1998). Early colorectal cancer: recognition, classification and treatment. *Br J Surg* **85**: 469–476.
7. Nivatvongs, S (2000). Surgical management of early colorectal cancer. *World J Surg* **24**: 1052–1055.
8. Ando, N, Ozawa, S, Kitagawa, Y, Shinozawa, Y and Kitajima, M (2000). Improvement in the results of surgical treatment of advanced squamous esophageal carcinoma during 15 consecutive years. *Ann Surg* **232**: 225–232.
9. Gotoda, T (2007). Endoscopic resection of early gastric cancer. *Gastric Cancer* **10**: 1–11.
10. Nascimbeni, R, Burgart, LJ, Nivatvongs, S and Larson, DR (2002). Risk of lymph node metastasis in T1 carcinoma of the colon and rectum. *Dis Colon Rectum* **45**: 200–206.
11. Wang, HS, Liang, WY, Lin, TC, Chen, WS, Jiang, JK, Yang, SH *et al.* (2005). Curative resection of T1 colorectal carcinoma: risk of lymph node metastasis and long-term prognosis. *Dis Colon Rectum* **48**: 1182–1192.
12. Takeuchi, H and Kitagawa, Y (2013). Sentinel node navigation surgery in patients with early gastric cancer. *Dig Surg* **30**: 104–111.
13. Kishimoto, H, Kojima, T, Watanabe, Y, Kagawa, S, Fujiwara, T, Uno, F *et al.* (2006). *In vivo* imaging of lymph node metastasis with telomerase-specific replication-selective adenovirus. *Nat Med* **12**: 1213–1219.
14. Burton, JB, Johnson, M, Sato, M, Koh, SB, Mulholland, DJ, Stout, D *et al.* (2008). Adenovirus-mediated gene expression imaging to directly detect sentinel lymph node metastasis of prostate cancer. *Nat Med* **14**: 882–888.
15. Liu, TC, Galanis, E and Kirn, D (2007). Clinical trial results with oncolytic virotherapy: a century of promise, a decade of progress. *Nat Clin Pract Oncol* **4**: 101–117.
16. Park, BH, Hwang, T, Liu, TC, Sze, DY, Kim, JS, Kwon, HC *et al.* (2008). Use of a targeted oncolytic poxvirus, JX-594, in patients with refractory primary or metastatic liver cancer: a phase I trial. *Lancet Oncol* **9**: 533–542.
17. Fujiwara, T (2009). Telomerase-specific virotherapy for human squamous cell carcinoma. *Expert Opin Biol Ther* **9**: 321–329.
18. Uchida, H, Marzulli, M, Nakano, K, Goins, WF, Chan, J, Hong, CS *et al.* (2013). Effective treatment of an orthotopic xenograft model of human glioblastoma using an EGFR-retargeted oncolytic herpes simplex virus. *Mol Ther* **21**: 561–569.
19. Kawashima, T, Kagawa, S, Kobayashi, N, Shirakiya, Y, Umeoka, T, Teraishi, F *et al.* (2004). Telomerase-specific replication-selective virotherapy for human cancer. *Clin Cancer Res* **10**(1 Pt 1): 285–292.
20. Hashimoto, Y, Watanabe, Y, Shirakiya, Y, Uno, F, Kagawa, S, Kawamura, H *et al.* (2008). Establishment of biological and pharmacokinetic assays of telomerase-specific replication-selective adenovirus. *Cancer Sci* **99**: 385–390.
21. Sasaki, T, Tazawa, H, Hasei, J, Kunisada, T, Yoshida, A, Hashimoto, Y *et al.* (2011). Preclinical evaluation of telomerase-specific oncolytic virotherapy for human bone and soft tissue sarcomas. *Clin Cancer Res* **17**: 1828–1838.
22. Kojima, T, Hashimoto, Y, Watanabe, Y, Kagawa, S, Uno, F, Kuroda, S *et al.* (2009). A simple biological imaging system for viable human circulating tumor cells. *J Clin Invest* **119**: 3172–3181.
23. Takeshita, K, Tani, M, Inoue, H, Saeki, I, Havashi, S, Honda, T *et al.* (1997). Endoscopic treatment of early oesophageal or gastric cancer. *Gut* **40**: 123–127.
24. Kojima, T, Parra-Blanco, A, Takahashi, H and Fujita, R (1998). Outcome of endoscopic mucosal resection for early gastric cancer: review of the Japanese literature. *Gastrointest Endosc* **48**: 550–4; discussion 554.
25. Inoue, H, Fukami, N, Yoshida, T and Kudo, SE (2002). Endoscopic mucosal resection for esophageal and gastric cancers. *J Gastroenterol Hepatol* **17**: 382–388.
26. Borie, F, Plaisant, N, Millat, B, Hay, JM and Fagniez, PL; French Associations for Surgical Research (2004). Appropriate gastric resection with lymph node dissection for early gastric cancer. *Ann Surg Oncol* **11**: 512–517.
27. Blackburn, EH (1991). Structure and function of telomeres. *Nature* **350**: 569–573.
28. Kim, NW, Piatyszek, MA, Prowse, KR, Harley, CB, West, MD, Ho, PL *et al.* (1994). Specific association of human telomerase activity with immortal cells and cancer. *Science* **266**: 2011–2015.
29. Gu, J, Andreeff, M, Roth, JA and Fang, B (2002). hTERT promoter induces tumor-specific Bax gene expression and cell killing in syngenic mouse tumor model and prevents systemic toxicity. *Gene Ther* **9**: 30–37.
30. Christiansen, A and Detmar, M (2011). Lymphangiogenesis and cancer. *Genes Cancer* **2**: 1146–1158.
31. Goel, S, Duda, DG, Xu, L, Munn, LL, Boucher, Y, Fukumura, D *et al.* (2011). Normalization of the vasculature for treatment of cancer and other diseases. *Physiol Rev* **91**: 1071–1121.
32. Hagendoorn, J, Tong, R, Fukumura, D, Lin, Q, Lobo, J, Padera, TP *et al.* (2006). Onset of abnormal blood and lymphatic vessel function and interstitial hypertension in early stages of carcinogenesis. *Cancer Res* **66**: 3360–3364.

33. Kume, K (2014). Endoscopic therapy for early gastric cancer: standard techniques and recent advances in ESD. *World J Gastroenterol* **20**: 6425–6432.
34. Uraoka, T, Saito, Y, Yamamoto, K and Fujii, T (2009). Submucosal injection solution for gastrointestinal tract endoscopic mucosal resection and endoscopic submucosal dissection. *Drug Des Devel Ther* **2**: 131–138.
35. Yamasaki, Y, Tazawa, H, Hashimoto, Y, Kojima, T, Kuroda, S, Yano, S *et al.* (2012). A novel apoptotic mechanism of genetically engineered adenovirus-mediated tumour-specific p53 overexpression through E1A-dependent p21 and MDM2 suppression. *Eur J Cancer* **48**: 2282–2291.
36. Nemunaitis, J, Tong, AW, Nemunaitis, M, Senzer, N, Phadke, AP, Bedell, C *et al.* (2010). A phase I study of telomerase-specific replication competent oncolytic adenovirus (telomelysin) for various solid tumors. *Mol Ther* **18**: 429–434.
37. Fujiwara, T, Tanaka, N, Kanazawa, S, Ohtani, S, Saijo, Y, Nukiwa, T *et al.* (2006). Multicenter phase I study of repeated intratumoral delivery of adenoviral p53 in patients with advanced non-small-cell lung cancer. *J Clin Oncol* **24**: 1689–1699.
38. Kojima, T, Watanabe, Y, Hashimoto, Y, Kuroda, S, Yamasaki, Y, Yano, S *et al.* (2010). *In vivo* biological purging for lymph node metastasis of human colorectal cancer by telomerase-specific oncolytic virotherapy. *Ann Surg* **251**: 1079–1086.
39. Kishimoto, H, Urata, Y, Tanaka, N, Fujiwara, T and Hoffman, RM (2009). Selective metastatic tumor labeling with green fluorescent protein and killing by systemic administration of telomerase-dependent adenoviruses. *Mol Cancer Ther* **8**: 3001–3008.
40. Kishimoto, H, Aki, R, Urata, Y, Bouvet, M, Momiyama, M, Tanaka, N *et al.* (2011). Tumor-selective, adenoviral-mediated GFP genetic labeling of human cancer in the live mouse reports future recurrence after resection. *Cell Cycle* **10**: 2737–2741.
41. Yang, M, Reynoso, J, Jiang, P, Li, L, Moossa, AR and Hoffman, RM (2004). Transgenic nude mouse with ubiquitous green fluorescent protein expression as a host for human tumors. *Cancer Res* **64**: 8651–8656.
42. Bouvet, M, Tsuji, K, Yang, M, Jiang, P, Moossa, AR and Hoffman, RM (2006). *In vivo* color-coded imaging of the interaction of colon cancer cells and splenocytes in the formation of liver metastases. *Cancer Res* **66**: 11293–11297.

Breast Cancer Res Treat
DOI 10.1007/s10549-015-3265-y

PRECLINICAL STUDY

Viral transduction of the HER2-extracellular domain expands trastuzumab-based photoimmunotherapy for HER2-negative breast cancer cells

Kyoko Shimoyama · Shunsuke Kagawa · Michihiro Ishida · Shinichiro Watanabe · Kazuhiro Noma · Kiyoto Takehara · Hiroshi Tazawa · Yuuri Hashimoto · Shunsuke Tanabe · Junji Matsuoka · Hisataka Kobayashi · Toshiyoshi Fujiwara

Received: 19 September 2014 / Accepted: 26 December 2014

Abstract The prognosis of HER2-positive breast cancer has been improved by trastuzumab therapy, which features high specificity and limited side effects. However, trastuzumab-based therapy has shortcomings. Firstly, HER2-targeted therapy is only applicable to HER2-expressing tumors, which comprise only 20–25 % of primary breast cancers. Secondly, many patients who initially respond to trastuzumab ultimately develop disease progression. To overcome these problems, we employed virus-mediated HER2 transduction and photoimmunotherapy (PIT) which involves trastuzumab conjugated with a photosensitizer, trastuzumab-IR700, and irradiation of near-infrared light. We hypothesized that the gene transduction technique together with PIT would expand the range of tumor entities suitable for trastuzumab-based therapy and improve its antitumor activity. The HER2-extracellular domain (ECD) was transduced by the adenoviral vector, Ad-HER2-ECD, and PIT with trastuzumab-IR700 was applied in the HER2-negative cancer cells. Ad-HER2-ECD can efficiently transduce HER2-ECD into HER2-negative human cancer cells. PIT with trastuzumab-IR700 induced direct cell membrane destruction of Ad-HER2-ECD-transduced HER2-negative cancer cells. Novel combination of viral transduction of a target antigen and an antibody-based PIT would expand and potentiate molecular-targeted therapy even for target-negative or attenuated cancer cells.

Keywords Photoimmunotherapy · HER2 · Breast cancer · Adenovirus

Abbreviations

DMEM	Dulbecco's modified Eagle's medium
ECD	Extracellular domain
HER2	Human epidermal growth factor receptor type 2
MOI	A multiplicity of infection
NIR	Near infrared
PBS	Phosphate-buffered saline
PI	Propidium iodide
PIT	Photoimmunotherapy
SDS	Sodium dodecyl sulfate
SQ	Self-quenched
Tra-IR700	Trastuzumab-IR700

Electronic supplementary material The online version of this article (doi:10.1007/s10549-015-3265-y) contains supplementary material, which is available to authorized users.

K. Shimoyama · S. Kagawa (✉) · M. Ishida · S. Watanabe · K. Noma · K. Takehara · H. Tazawa · Y. Hashimoto · S. Tanabe · T. Fujiwara
Department of Gastroenterological Surgery, Okayama University Graduate School of Medicine, Dentistry and Pharmacological Sciences, 2-5-1 Shikata-cho, Kita-ku, Okayama 700-8558, Japan
e-mail: skagawa@md.okayama-u.ac.jp

H. Tazawa
Center for Innovative Clinical Medicine, Okayama University Hospital, Okayama, Japan

J. Matsuoka
Department of Palliative Care, Okayama University Hospital, Okayama, Japan

H. Kobayashi
Molecular Imaging Program, Center for Cancer Research, National Cancer Institute, US National Institutes of Health, Bethesda, MD, USA

Published online: 24 January 2015

XTT The sodium 3′-[1-(phenylaminocarbonyl)-3,4-tetrazolium]-bis(4-methoxy-6-nitro) benzene sulfonic acid hydrate

Introduction

HER2 is a well-known oncogene, the overexpression of which is strongly associated with more aggressive tumors and poorer overall survival [1]. Strategies such as trastuzumab that target HER2 have greatly improved the prognosis of HER2-positive breast cancer through their high specific targeting ability [2]. However, the clinical efficacy of HER2-targeted therapy is limited to breast cancers that overexpress HER2, which only account for 20–30 % of all breast cancer [3, 4] and which are also inclined to develop resistance [5]. In addition, although trastuzumab is known to have few side effects apart from cardiac toxicity, trastuzumab is usually used together with an anti-tumor drug [6, 7], because its effect is not strong enough when used as a sole agent.

Photoimmunotherapy (PIT) was developed as a new type of molecular-targeted cancer therapy. PIT uses specific monoclonal antibodies that are targeted toward cell surface receptors and that are conjugated to the photosensitizer phthalocyanine dye, IR700, which is cytotoxic upon irradiation with near-infrared (NIR) light [8]. Trastuzumab-IR700 (Tra-IR700) was designed to specifically target HER2-expressing cells. Cell death is only induced when the cells are bound by Tra-IR700 and irradiated with NIR light. Death is presumably induced by cell membrane damage due to local expansion of heated water [8].

Modified adenovirus type 5 vectors have been widely used as a platform for the delivery of genes of interest into various types of human cells. In a previous study, we constructed a replication-deficient adenoviral vector containing a gene that encodes the HER2 extracellular domain (Ad-HER2-ECD) [9]. We demonstrated that infection with Ad-HER2-ECD resulted in expression of the HER2-ECD on the surface of HER2-negative or trastuzumab-resistant HER2-attenuated cancer cells. The expressed HER2-ECD did not trigger HER2 signaling pathways because of the lack of the HER2 intracellular kinase domain [9].

We hypothesized that if the Ad-HER2-ECD-mediated gene transduction technique was used together with molecular-targeted cancer therapy using PIT, the range of tumor entities suitable for trastuzumab-based therapy would be expanded and the problem of resistance and narrow indication could be overcome.

Materials and methods

Cell lines and cell cultures

Three human mammary gland adenocarcinoma cell lines, SKBR3, MDA-MB-231, and MCF7, were obtained from the American Type Culture Collection. SKBR3, MDA-MB-231, and MCF7 were cultured in McCoy's 5A medium, Leibovitz's L-15 Medium, and Dulbecco's modified Eagle's medium (DMEM) supplemented with 2 mmol/ml L-glutamine, respectively. The human osteosarcoma cell line Saos-2 was kindly provided by Dr. Kyo (Kanazawa University, Ishikawa, Japan), and the cells were propagated as monolayer cultures in DMEM. Penicillin (100 units/ml), streptomycin (100 μg/ml), and 10 % fetal bovine serum were added to the medium. The cells were maintained at 37 °C in a humidified atmosphere with 5 % CO_2.

Recombinant adenovirus

A replication-deficient adenoviral vector expressing the extracellular and trans-membrane domains of HER2 (Ad-HER2-ECD) was constructed [9]. Briefly, the HER2-ECD expression cassette, which contains the human cytomegalovirus promoter, HER2-ECD cDNA, and the SV40 early polyadenylation signal, was inserted between the XbaI and ClaI sites of pXCJL.1. The HER2-ECD shuttle vector and the recombinant plasmid pJM17 were cotransfected into 293 cells. The culture supernatant of 293 cells that showed the complete cytopathic effect, which contained virus progenies, was collected and used for subsequent production. The resultant virus was purified by ultracentrifugation in cesium chloride step gradients, and its titer was determined by a plaque-forming assay using 293 cells. The virus was stored at −80 °C until use. Ad-GFP was used as a control adenovirus [10].

Western blotting analysis

Primary antibodies against HER2-ECD (Ab-20, Thermo Scientific) and β-actin (AC-15, Sigma Chemical, Co.) were used. Proteins were electrophoretically transferred to Hybond-polyvinylidene difluoride transfer membranes (GE Healthcare Life Science), incubated with primary antibody and then with peroxidase-linked secondary antibody according to the manufacturer's protocol. The Amersham ECL chemiluminescence system (GE Healthcare Life Science) was used to detect the peroxidase activity of the bound antibody. In experiments with replication-deficient adenoviral vector, cells were infected with Ad-HER2-ECD or Ad-GFP at a multiplicity of infection (MOI) of 50 for 48 h.

Flowcytometric analysis

To measure the expression of HER2-ECD in cells infected with Ad-HER2-ECD, cells were labeled with APC-conjugated mouse monoclonal anti-HER2-ECD antibody (R&D Systems Inc.) or APC-conjugated IgG2b as control (Miltenyi Biotec, Inc.) on ice for 45 min and were then analyzed using a FACS instrument (BD Biosciences). The intensity of staining was determined using the BD-FACS Software (Flow Jo 7.6.1).

Immunocytochemistry

Cells cultured on 4 chamber glass slides were fixed with 4 % paraformaldehyde in PBS for 15 min and blocked with 3 % bovine serum albumin for 30 min. Slides were then labeled with APC-conjugated mouse monoclonal anti-HER2-ECD antibody (R&D Systems Inc.) on ice for 45 min and were subsequently photographed using a Confocal Laser Scanning Biological Microscope with a 647-nm excitation filter (FV10i, Olympus, Tokyo, Japan).

Synthesis of IR700-conjugated trastuzumab

Trastuzumab was obtained from Chugai Pharmaceutical Co. The IR700 dye (LI-COR Biosciences) was conjugated to trastuzumab following the manufacturer's instructions. Briefly, trastuzumab (1 mg) was incubated with IR700 (66.8 mg, 34.2 nmol, 5 mmol/L in DMSO) in 0.1 mol/L Na_2HPO_4 (pH 8.6) at room temperature for 1 h. Conjugated Tra-IR700 was purified using a Sephadex G50 column (PD-10; GE Healthcare). Protein concentrations were determined using a Coomassie Plus Protein Assay Kit (Pierce Biotechnology) by measurement of light absorption at 620 nm (8453 Value System; Agilent Technologies).

Fluorescence microscopy

To detect specific antigen-mediated localization of IR700 on the surface of MCF7 and MDA-MB-231 cells, the cells were seeded at 2×10^4/well on cover glass-bottomed dishes, incubated for 24 h, and infected with Ad-HER2-ECD at an MOI of 50 for 48 h. Tra-IR700 (10 μg/ml) was then added to the culture medium and incubated for 6 h at 37 °C. The cells were washed with PBS and fluorescence was observed under a Confocal Laser Scanning Biological Microscope (FV10i, Olympus, Japan) with a 647-nm excitation filter.

In vitro Photoimmunotherapy

Cells were seeded on 35 mm cell-culture dishes at 2×10^4/well or 96-well black plates at 5×10^3/well, and were infected with Ad-HER2-ECD or Ad-GFP at an MOI of 50 for 48 h. The medium was then replaced with fresh culture medium containing 10 μg/ml of Tra-IR700 and was further incubated for 6 h at 37 °C. After washing with PBS, the cells were then irradiated with light from a red light-emitting diode at wavelengths of 670–690 nm for 35 mm cell-culture dishes and at a wavelength of 625 nm for 96-well black plates. The filter set to detect IR700 when observed under a fluorescence microscope (IX71; Olympus, Tokyo, Japan) consisted of a 590–650-nm excitation filter and a 665–740-nm band pass emission filter. Power density ranged from 40 to 100 mW/cm^2, as measured using an optical power meter (PM 100, Thorlabs, Inc.).

Cell viability assay

Cell viability was determined 3 days after PIT using the Cell Proliferation Kit II (Roche Molecular Biochemicals) with the sodium 3′-[1-(phenylaminocarbonyl)-3,4-tetrazolium]-bis (4-methoxy-6-nitro) benzene sulfonic acid hydrate (XTT) assay, according to the manufacturer's protocol. Propidium iodide (PI), which is plasma membrane impermeable, was used to stain membrane-disrupted dead cells [11]. PI was added to the medium at an approximate final concentration of 1 μg/mL and was incubated at 37 °C for 30 min.

Statistical analysis

A comparison of continuous variables between two groups for in vitro assays was performed using the two-sided Student's t test. Differences between groups were considered to be statistically significant when the p values were <0.05.

Results

HER2-ECD expression induced by Ad-HER2-ECD

MCF7 and MDA-MB-231 breast cancer cells were chosen as HER2 negative breast cancer lines since their expression of HER2 is known to be almost negative, or barely detectable [12]. Initially, Ad-GFP was used as a substitute for Ad-HER2-ECD in preliminary experiments aimed at finding the optimal dose of Ad-HER2-ECD to transduce HER2-ECD into these cells and at examining the transduction efficiency of the adenovirus. We found that an MOI of 50 was the optimal MOI, at which almost all cells were transduced with GFP proteins without cellular toxicity (Supplementary Fig. 1). Based on these data, HER2-negative breast cancer cells were infected with Ad-HER2-ECD at an MOI of 50 for 48 h, to transduce HER2-ECD.

Western blot analysis showed that Ad-HER2-ECD infection resulted in a marked increase in the expression of the 100-kDa HER2-ECD protein in HER2 low-expressing MCF7 and MDA-MB-231 breast cancer cells as compared to parental cells and Ad-GFP-infected cells (Fig. 1a). Flowcytometric analysis further demonstrated the expression of HER2-ECD on the cell surface (Fig. 1b). The cell surface expression of HER2-ECD in Ad-HER2-ECD-infected cells was also confirmed using immunocytochemistry (Fig. 1c).

Trastzumab-IR700 binds to the transduced HER2-ECD

We next examined whether Tra-IR700 bound to the HER2-ECD that was overexpressed on MCF7 and MDA-MB-231 cells by Ad-HER2-ECD transduction. Because IR700 is fluorescent, it can be directly detected by fluorescence microscopy allowing visualization of the cellular location of bound Tra-IR700 conjugates. MCF7 and MDA-MB-231 cells were transduced with HER2-ECD using Ad-HER2-ECD and the cells were then incubated with Tra-IR700 for 6 h. Fluorescent imaging confirmed that Tra-IR700 primarily bound to the cell surface of infected, HER2-ECD-transduced cells (Fig. 2).

Morphological changes in Ad-HER2-ECD-infected HER2-negative cells after trastuzumab-IR700 with PIT

The effects of Tra-IR700 and PIT treatment on the cell morphology of Ad-HER2-ECD-infected breast cancer cells over time were microscopically examined. Two different types of morphological changes were observed in MCF7 and MDA-MB-231 cells after irradiation with NIR light. In MCF-7 cells, bubbling at the cell surface

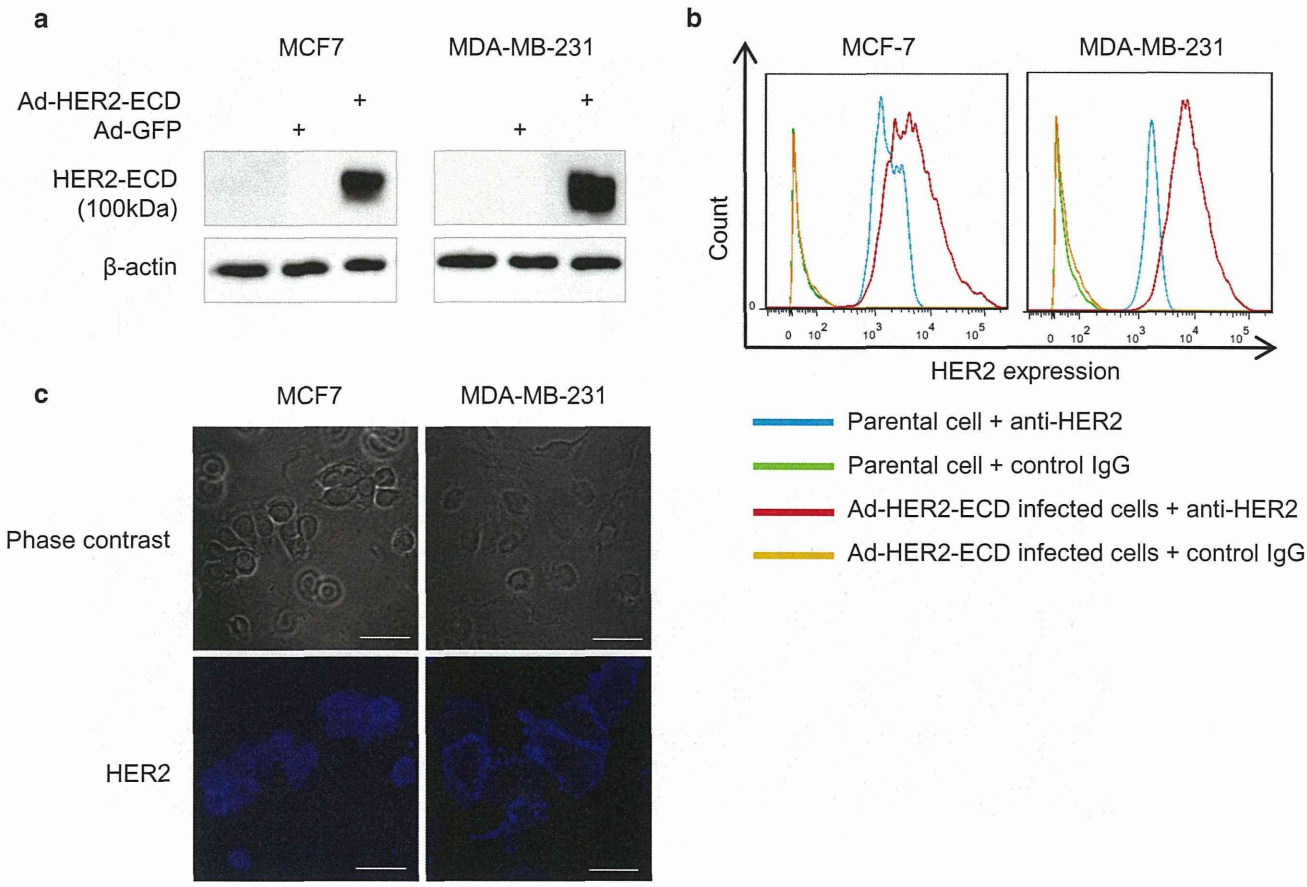

Fig. 1 HER2-extracellular domain (ECD) expression induced by Ad-HER2-ECD. **a** Western blot analysis showing expression of the 100-kDa HER2-ECD protein in Ad-HER2-ECD-infected cells but not in Ad-GFP-infected or parental cells. Actin was used as a loading control. **b** Flowcytometric analysis showing HER2-ECD expression on the cell membrane. Cells were labeled with APC-conjugated mouse monoclonal anti-HER2-ECD antibody (*blue* and *red*) or APC-conjugated IgG2b as a negative control (*green* and *yellow*). **c** Immunocytochemical analysis of the cell surface expression of HER2-ECD on Ad-HER2-ECD-infected cells using an APC-conjugated anti-HER2-ECD antibody. *Scale bars* 50 μm

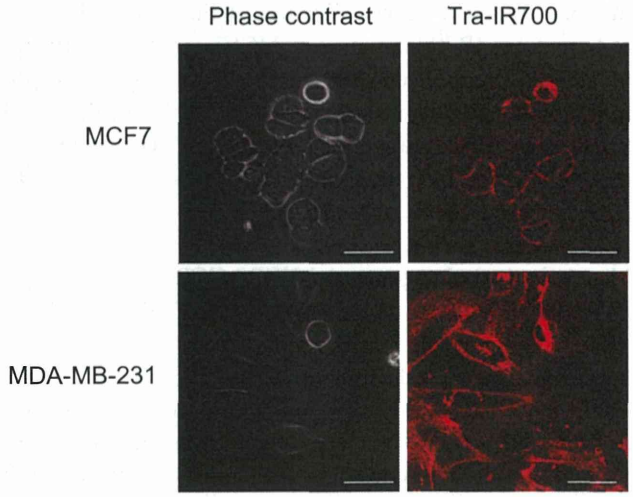

Fig. 2 Trastzumab-IR700 binds to the transduced cell surface HER2-ECD Immunofluorescent analysis of Trastzumab-IR700 (Tra-IR700) binding to HER2-ECD-transduced by Ad-HER2-ECD on the cell surface of breast cancer cells. *Scale bars* 50 μm

preceded total cell shrinkage. In MDA-MB-231 cells in contrast, instead of bubbling, many granules appeared in the cytoplasm, followed by shrinkage of the cells (Fig. 3a). Of note, these changes were observed within 1 min after irradiation with NIR light. A higher amount of light (18 J) resulted in more exaggerated changes in morphology than a lower amount of light (6 J) (Fig. 3a). Ad-HER2-ECD-infected cells died within 72 h after Tra-IR700 with PIT (6 J), while untreated cells and Ad-GFP-infected cells survived (Fig. 3b). These phenomena were captured as time-lapse movies (Supplementary movies 1, 2). We further confirmed cell death of the MCF7 and MDA-MD-231 cells at 72 h after irradiation with NIR light (18 J) by staining of cells whose membranes had been destroyed using PI staining (Fig. 3c). Morphological change and PI staining of cells immediately following PIT were also reproduced in Ad-HER2-ECD-infected and PIT-treated HER2 negative osteosarcoma Saos-2 cells (Supplementary Fig. 2).

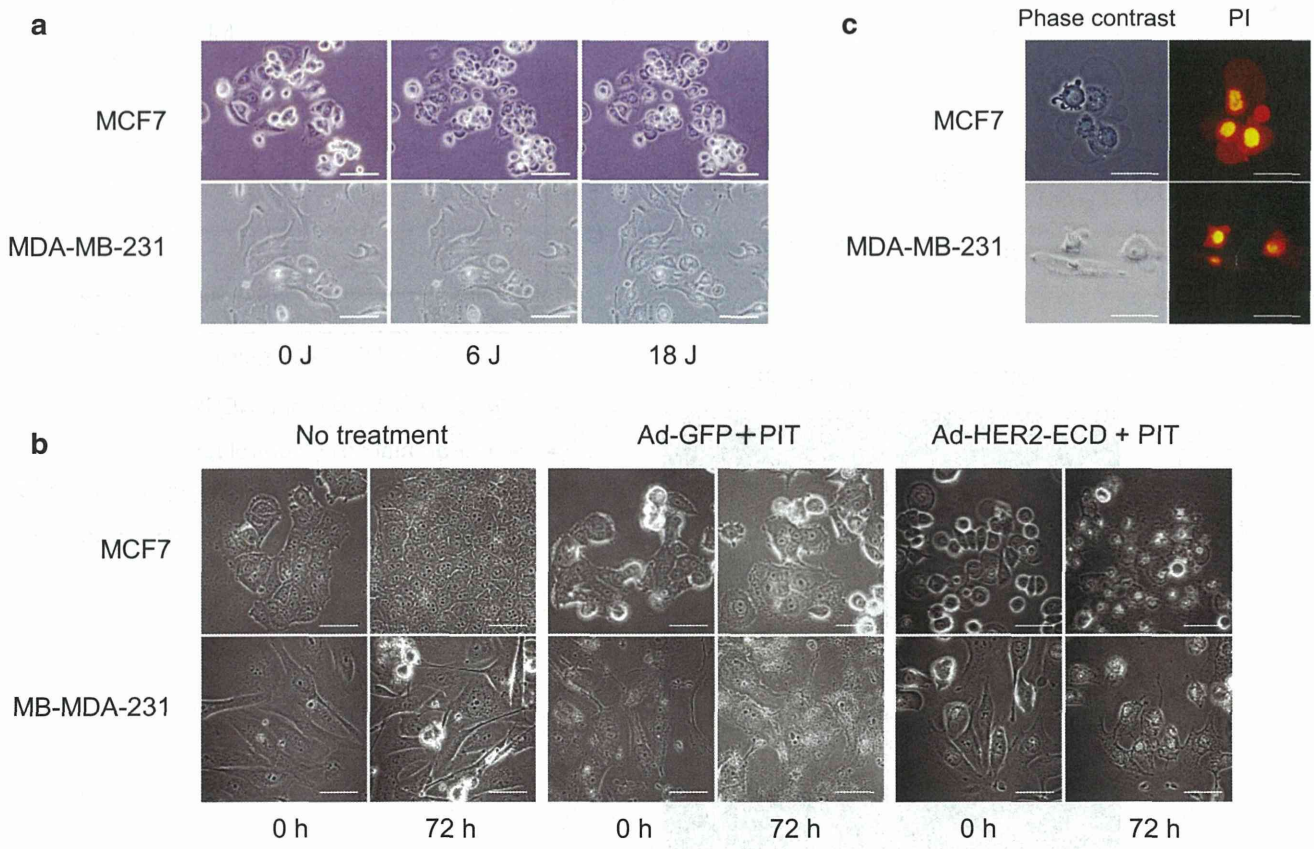

Fig. 3 Microscopic analysis of the effect of Tra-IR700-mediated PIT on the cell morphology and cell death of HER2-ECD-transduced HER2-negative cells. **a** Phase contrast analysis of the morphology of the breast cancer cells MCF-7 and MDA-MB-231 immediately following PIT using 0, 6, or 18 J. *Scale bars* 50 μm. **b** Phase contrast analysis of control, Ad-GFP-infected or Ad-HER2-ECD-infected MCF-7 and MDA-MB-231 cells before and after 72 h treatment with Tra-IR700-mediated PIT using 6 J. Ad-HER2-ECD-infected cells but not the other cells displayed cell shrinkage. *Scale bars* 50 μm. **c** Analysis of cell death of HER2-ECD-transduced cells following Tra-IR700-mediated PIT (12 J) 72 h after treatment. The PI staining indicates that plasma membrane destruction was induced by the treatment. *Scale bars* 50 μm

Quantitative evaluation of the cytotoxicity of Trastuzumab-IR700 with PIT for Ad-HER2-ECD-infected HER2 negative cells

The specific cytotoxicity of anti-HER2 PIT was quantitatively evaluated using the XTT assay of cell viability and HER2-transduced MCF7 and MDA-MB-231 cells (Fig. 4a, b). Treatment included seven control conditions in addition to Ad-HER2-ECD plus PIT. Only under the treatment condition that employed Ad-HER2-ECD together with Tra-IR700 mediated PIT (24 J for MDA-MB-231 and 36J for MCF-7), cell proliferation was significantly suppressed. In contrast, no significant cytotoxicity was observed under any other condition. Ad-HER2-ECD, Tra-IR700, or NIR irradiation did not harm the cells when each modality was given alone. HER2-specific cytotoxicity of Tra-IR700-mediated PIT was also reproduced in the HER2-positive breast cancer cell, SK-BR-3, and in Ad-HER2-ECD-infected Saos-2 cells (Supplementary Fig. 3a, b). These results indicated that Tra-IR700-mediated PIT selectively and specifically targets HER2-ECD-transduced cancer cells.

Discussion

Over the past decades, research has transformed the care of patients with breast cancer through the application of basic science to the clinic [13]. Monoclonal antibodies currently occupy a key position among anti-cancer drugs due to their high specificity and efficacy, which can be achieved in spite of their low side effects. The typical clinical approach for HER2-positive breast cancer has been altered since the approval of trastuzumab [13]. However, for such molecular-targeted therapy, the indication is limited to the populations which express the specific target antigen. In order to overcome this issue, we tried to artificially express the target antigen in target-negative cancer cells by viral transfection. We proved that viral transduction of HER2-ECD made even HER2-negative breast cancer cells sensitive to anti-HER2 photoimmunotherapy. Thus, this technique could expand the indication of antibody-directed therapy to not only target-positive but also to target-negative cancers.

In the present study, we have reproducibly expressed HER2-ECD on the cell membrane of HER2-negative MCF7 and MDA-MB-231 cells, as evidenced by immunocytochemistry as well as by flow cytometry. Although flow cytometric analysis suggested that both parental MCF7 and MDA-MB-231 cells express HER2, the 185 kDa HER2 protein could not be detected in these parental cells by Western blot analysis. These results are consistent with previous reports by other groups, which demonstrated that the levels of HER2 expression in these cell lines are low or negligible and that these cell lines are not sensitive to anti-HER2 therapy [14–16].

In addition to confirmation of HER2-ECD expression, we also confirmed that Tra-IR700 bound directly to transduced HER2-ECD by observation under a confocal fluorescence microscope. Since IR700 itself emits fluorescence [17] (Fig. 2), Tra-IR700 proved to be a useful agent not only for treatment, but also for monitoring [17–19]. In

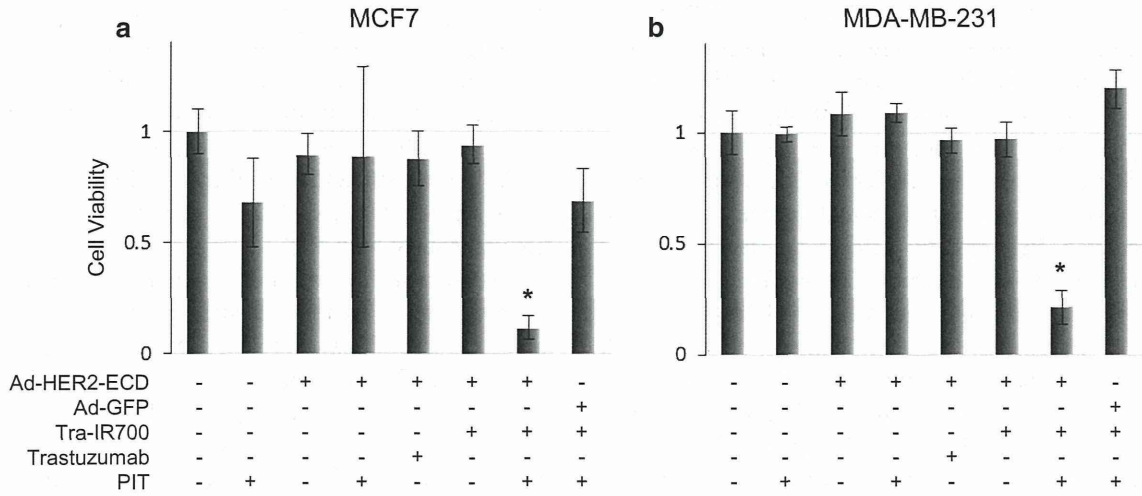

Fig. 4 Effect of Tra-IR700 mediated PIT treatment of HER2-ECD transduced HER2-negative cells on cell viability. Tra-IR700-mediated PIT was applied to the indicated cells along with seven control conditions and cell viability was quantified 72 h after PIT (24 J for MDA-MB-231 and 36 J for MCF-7) using the XTT assay. Only the group of Ad-HER2-ECD-infected cells treated with Tra-IR700-mediated PIT showed target-specific cell death. ($n = 4$, $^*p < 0.05$ for Tra-IR700-mediated PIT treatment compared to control groups using Student's t test.)